Optical Gain and Stimulated Emission in Nanocrystal Quantum Dots

V. I. Klimov,[1]* A. A. Mikhailovsky,[1] Su Xu,[1] A. Malko,[1]
J. A. Hollingsworth,[1] C. A. Leatherdale,[2] H.-J. Eisler,[2]
M. G. Bawendi[2]*

The development of optical gain in chemically synthesized semiconductor nanoparticles (nanocrystal quantum dots) has been intensely studied as the first step toward nanocrystal quantum dot lasers. We examined the competing dynamical processes involved in optical amplification and lasing in nanocrystal quantum dots and found that, despite a highly efficient intrinsic nonradiative Auger recombination, large optical gain can be developed at the wavelength of the emitting transition for close-packed solids of these dots. Narrowband stimulated emission with a pronounced gain threshold at wavelengths tunable with the size of the nanocrystal was observed, as expected from quantum confinement effects. These results unambiguously demonstrate the feasibility of nanocrystal quantum dot lasers.

Semiconductor lasers have become ubiquitous. Both optically and electrically pumped lasers are widely used in fields ranging from telecommunications and information storage and processing to medical diagnostics and therapeutics. The use of semiconductor quantum well (QW) structures as optical gain media has resulted in important advances in semiconductor laser technology (*1, 2*). Quantum confinement in one dimension restricts carrier motion in QWs to the remaining two dimensions. Consequently, QWs have a two-dimensional steplike density of electronic states that is nonzero at the band edge, enabling a higher concentration of carriers to contribute to the band-edge emission and leading to a reduced lasing threshold, improved temperature stability, and a narrower emission line.

A further enhancement in the density of states at the band edge and an associated reduction in the lasing threshold is, in principle, possible with quantum wires and quantum dots (QDs), where the quantum confinement is in two and three dimensions, respectively (*3, 4*). The electronic spectrum of QDs consists of well-separated atomic-like states with an energy spacing that increases as the dot size is reduced (*5, 6*). In very small QDs, the spacing of the electronic states is much greater than the available thermal energy (strong confinement), inhibiting thermal depopulation of the lowest electronic states, which should result in a lasing threshold that is temperature-insensitive at an excitation level of only one electron-hole (e-h) pair per dot on average (*4*). Additionally, QDs in the strong confinement regime have an emission wavelength that is a pronounced function of size, adding the advantage of continuous spectral tunability over a wide energy range simply by changing the size of the dots. The prospect of realizing QD lasers for which the output color can be controlled by facile manipulation of QD size and semiconductor composition has been a driving force in nanocrystal QD research for more than a decade.

Lasing has previously been demonstrated for epitaxially group III-V QDs (*7–9*). These dots have relatively large lateral sizes (typically >10 nm); therefore, the spacing between their electronic states is smaller than room temperature carrier energies (weak confinement), and the lasing threshold is temperature sensitive. Further, large lateral dimensions and difficulties in size control limit their spectral tunability using quantum confinement effects. As a result, the emission wavelengths in epitaxial dots are usually controlled by a material's composition rather than by the QD size (*9*).

An alternative approach to fabricating QDs that are small enough to show strong quantum confinement is through chemical synthesis. Chemical methods can provide routine preparations of semiconductor nanoparticles (nanocrystal QDs) with radii from 1 to 6 nm and with size dispersions as small as 5% (*10*). In this size range, electronic interlevel spacings can exceed hundreds of meV, and size-controlled spectral tunability over an energy range as wide as 1 eV can be achieved. Additionally, nanocrystal QDs can be chemically manipulated like large molecules. They can be incorporated into polymer and glass matrices and into different photonic structures, including microcavities and photonic crystals. Nanocrystal QDs can also be assembled into close-packed ordered and disordered arrays (QD solids) (*11*). The combination of tunable electronic energies and chemical flexibility makes nanocrystal QDs ideal building blocks for the bottom-up assembly of optical device structures, including optical amplifiers and lasers.

There are substantial differences between the electronic and optical properties of nanocrystal QDs and those of epitaxial dots, mostly due to the smaller size of nanocrystal QDs. In particular, strong quantum confinement in nanocrystal QDs results in a large splitting of band-edge states (*12, 13*) and in an enhancement of intrinsic nonradiative Auger recombinations (*14*). Both of these effects are critical for understanding and observing optical amplification in nanocrystal QDs.

Although optical gain in nanocrystal QDs of CdSe and CdS grown in glass matrices has been reported (*15–18*), narrowband stimulated emission was only demonstrated for large dots (radius $R \sim 7$ nm) (*15*), comparable in size to epitaxial dots and beyond the desired strong confinement regime. The difficulties in achieving stimulated emission in glass samples are due in part to the poor surface passivation of QDs, which leads to high rates of surface trapping and, consequently, to large nonradiative carrier losses. Large size distributions (~20 to 25%) and low loading levels further hinder the achievement of gain having a magnitude that is sufficient to compete with optical losses.

Direct chemical synthesis can produce colloidal QDs with narrow size distributions and improved surface passivation (*10*). For example, overcoating a core QD of CdSe with a shell of ZnS (*19, 20*) substantially suppresses surface trapping and produces room temperature photoluminescence (PL) quantum efficiencies as high as 50% with emission wavelengths tunable across the entire visible spectrum. However, despite more than a decade of attempts, stimulated emission had not been observed in colloidal QDs in the regime of strong confinement, where emission color depends on the size of the dot. In this report, we analyze the underlying physics of processes relevant to optical amplification and lasing in strongly confined nanocrystal QDs. We use femtosecond (fs) transient absorption (TA) and time-resolved PL to investigate the dynamical processes leading to buildup and decay of the optical gain. We show that there are intrinsic mechanisms that complicate the development of stimulated emission in strongly confined QDs but do not inherently prevent it. Further, we demonstrate optical gain and stimulated emission in close-packed films

---

[1] Chemistry Division, C-6, MS-J585, Los Alamos National Laboratory, Los Alamos, NM 87545, USA. [2] Department of Chemistry and Center for Materials Science and Engineering, Massachusetts Institute of Technology, 77 Massachusetts Avenue, Cambridge, MA 02139, USA.

*To whom correspondence should be addressed. E-mail: klimov@lanl.gov (V.I.K.) and mgb@mit.edu (M.G.B.)

of CdSe nanocrystal QDs in the strong confinement regime, highlighting spectral tunability with size.

Competition between radiative and nonradiative processes crucially affects optical gain. In nanocrystal QDs, nonradiative carrier losses are dominated by surface trapping and multiparticle Auger relaxation (*21*). If we model the band-edge emission in QDs using a two-level system with twofold spin-degenerate states, we find that optical gain (i.e., population inversion) begins at a carrier density of $N_{eh} = 1$ (N_{eh} is the number of e-h pairs per dot on average), with gain saturation (i.e., complete population inversion) at $N_{eh} = 2$. This implies that the QD band-edge gain is primarily due to two e-h pair states. For moderately well passivated dots, nonradiative Auger relaxation of doubly excited nanoparticles (τ_2) dominates over surface trapping and imposes an intrinsic limit on the lifetime of the optical gain in strongly confined QDs. In CdSe nanocrystal QDs, τ_2 is strongly size-dependent (approximately proportional to R^3) (*14*), shortening from 360 to 6 ps as the radius decreases from 4.1 to 1.2 nm. Because of this strong size dependence, Auger effects, which play a minor role in large epitaxial dots, become decisive in strongly confined nanocrystal QDs. The dominance of the Auger effect in nanocrystal QDs also implies that even relatively poorly passivated samples could behave as well as the best samples when it comes to gain and stimulated emission, because as long as trapping rates are lower than Auger rates, the two e-h pair lifetime is determined by the intrinsic Auger decay. The PL quantum efficiency of the sample, an indicator of QD surface passivation quality, may not be as important a factor for achieving lasing as initially thought.

When QDs are pumped into high-energy excited states, population inversion and the buildup of optical gain are only possible if the relaxation down to the emitting (ground) state is faster than the Auger process time τ_2. In CdSe dots, electron relaxation into the lowest 1S state [for notation of QD states, see, e.g., (*13*)] occurs with sub-ps time constants (*22*), which is much faster than τ_2. In order to measure the rate of the hole relaxation, we used a fs up-conversion time-resolved PL experiment (*23*). The continuous wave (cw) emission in colloidal QDs recorded under nonresonant excitation is red-shifted with respect to the lowest 1S absorption maximum (Fig. 1A). This shift is thought to be due to a splitting of the lowest hole state as a result of crystal field and e-h exchange interactions (*12, 13*). The high-energy fine-structure hole states are coupled to the 1S electron state by a strong transition that gives rise to an intense 1S absorption peak (Fig. 1B). The low-energy fine-structure state is responsible for the cw PL through a weaker transition. Hole relaxation from the "absorbing" to the "emitting" state is required for population buildup of the emitting transition and hence for the buildup of the optical gain.

The PL dynamics for QDs with $R = 1.2$ nm (Fig. 1C) recorded at the positions of the 1S absorption (the absorbing transition) and the PL maximum (the emitting transition) show a rapid (700 fs) decay of the 1S emission that is complementary to the growth of the emission at the center of the cw PL band (*24*). This indicates a fast sub-ps hole transition from the absorbing to the emitting state. Therefore, both electron and hole intraband relaxations in nanocrystal QDs are sufficiently fast to successfully compete with the Auger effect.

Development of optical gain and its dynamics were observed in a fs TA experiment. The light amplification/attenuation of the QD sample was probed with broadband pulses of a fs white light continuum variably delayed with respect to pump pulses. Optical gain was observed in TA spectra as an absorption bleach (absorption changes $\Delta\alpha < 0$) with a magnitude that is greater than that of the linear absorption (α_0) (i.e., $-\Delta\alpha/\alpha_0 > 1$). In our previous studies of QDs dispersed in hexane (*25*), we did not observe development of gain at the position of the 1S absorption band. This is consistent with Fig. 1C, indicating a fast hole relaxation from the absorbing state to a lower energy emitting state. We also did not detect gain at emission energies. Instead, a photoinduced absorption (PA) band rapidly developed below the 1S absorption resonance (dashed line in Fig. 1D). Analysis of TA data for QDs in different liquid and solid state matrices, shows that the PA below the 1S resonance strongly depends on the matrix material, indicating that it is probably due to excited-state absorption involving interface states. In QDs prepared as close-packed films or as dispersions in polyvinyl butyral, the PA band is reduced in magnitude and is red-

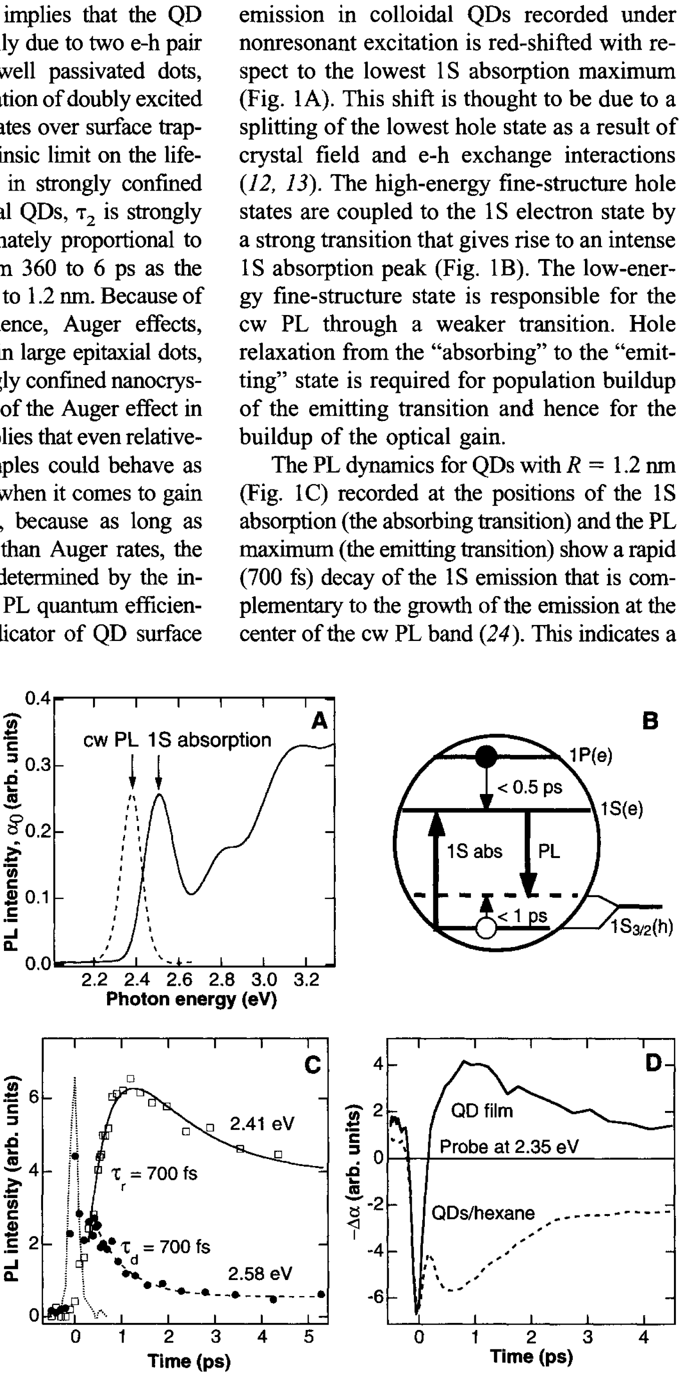

Fig. 1. (**A**) Absorption and cw PL spectra of CdSe QDs with $R = 1.2$ nm ($T = 300$ K). (**B**) Schematics of "absorbing" and "emitting" transitions in CdSe QDs along with intraband relaxation processes leading to a population buildup of the "emitting" transition. (**C**) Complementary PL dynamics detected at the positions of the absorbing (circles) and the emitting (squares) transitions (dotted line is a pump pulse autocorrelation). (**D**) TA dynamics at the position of the emitting transition for QDs dissolved in hexane (dashed line) and QDs prepared in the form of a close-packed film (solid line). The samples were pumped by frequency-doubled pulses from an amplified Ti-sapphire laser (3-eV photon energy, 100-fs pulse duration) operating at a 1-kHz repetition rate.

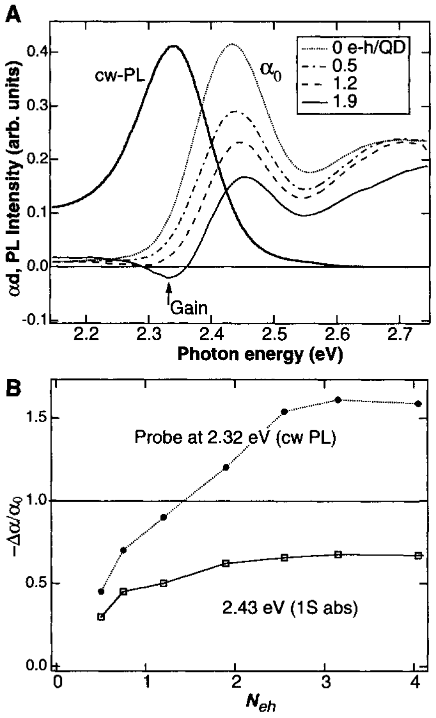

Fig. 2. (**A**) Development of optical gain in pump-dependent nonlinear absorption spectra for a CdSe nanocrystal QD film ($R = 1.3$ nm, $T = 300$ K). (**B**) Pump dependence of normalized absorption changes ($-\Delta\alpha/\alpha_0$) measured at the positions of the 1S absorption (squares) and cw PL (circles) bands.

shifted with respect to the PL band. As a result, these samples do not show excited-state absorption at the position of the emitting transition, but rather, they show a bleaching that turns into optical gain at sufficiently high carrier densities (solid line in Fig. 1D). The accidental overlap of pump-induced absorption with the PL band may explain the numerous unsuccessful attempts to detect gain and stimulated emission in solutions of nanocrystal QDs, including our own previous effort (*25*).

Figure 2A shows nonlinear absorption spectra ($\alpha = \alpha_0 + \Delta\alpha$) recorded at different excitation densities for a film of close-packed QDs with $R = 1.3$ nm (*26*). An increasing bleaching of the band-edge absorption with increased pump power is observed over the entire 1S band. However, a crossover from absorption to optical gain only occurs on the long-energy wing of the band at spectral energies corresponding to the cw PL band. Figure 2B shows the pump dependence of the normalized absorption changes ($-\Delta\alpha/\alpha_0$) at 2.43 eV (the 1S absorption maximum) and at 2.32 eV (the cw PL maximum). At pump intensities where $N_{eh} > 1$ (*27*), the 1S absorption bleaching saturates at $-\Delta\alpha/\alpha_0 \sim 0.7$, below the transition to optical gain, which is similar to our previous results for solution samples (*25*). On the other hand, the signal detected at the position of the emission band does show a crossover to optical gain ($-\Delta\alpha/\alpha_0 > 1$). The gain threshold is estimated to be close to one e-h pair per dot on average ($N_{eh} \sim 1.4$), consistent with a population-inversion mechanism in a simple two-level system. The maximum gain (G) measured for 1.3-nm dots is 510 cm^{-1}, giving a gain cross section ($\sigma_g = G/n_0$, where n_0 is the QD density in the sample) of $\sim 2 \times 10^{-17}$ cm^2.

We observed development of gain in solid state samples prepared from both QDs passivated with trioctylphosphine oxide (TOPO) (TOPO-capped) and QDs overcoated with a shell of ZnS (ZnS-capped). Figure 3 shows an example of normalized nonlinear absorption (gain) spectra for two TOPO-capped samples with QD radii of 1.3 and 2.1 nm and a ZnS-capped sample with $R = 1.7$ nm. All samples showed optical gain at the position of the emitting transition with a threshold estimated to be close to the theoretical limit of one e-h pair per dot on average, independent of dot size. The gain threshold in terms of the pump fluence scales roughly as R^3, as expected from the R^3 scaling of QD absorption cross sections (*21*). The data in Fig. 3 also illustrate the spectral tunability of gain with QD size: the gain band shifts by ~300 meV with a change in the dot radius from 2.1 to 1.3 nm.

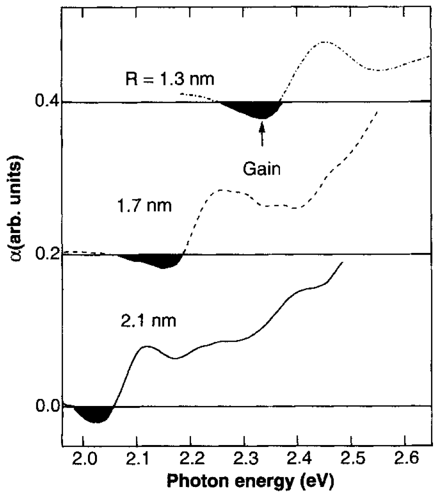

Fig. 3. Nonlinear absorption (gain) spectra of three QD film samples with R = 1.3, 1.7, and 2.1 nm recorded at 1.5 ps after excitation (T = 300 K).

The existence of optical gain, however, does not guarantee the development of stimulated emission. Stimulated emission can only be observed if its buildup time is faster than the gain relaxation. The stimulated emission buildup time is inversely proportional to the gain magnitude $\tau_s = n_r/(Gc)$, where c is the light velocity and n_r is the sample refractive index. This expression can be rewritten in terms of a gain cross section and the volume fraction of semiconductor material in the sample ($\xi = 4\pi n_0 R^3/3$)

$$\tau_s = \frac{4\pi R^3}{3}\frac{n_r}{\xi\sigma_g c} \qquad (1)$$

Assuming that the gain decay is dominated by the intrinsic two-pair Auger recombination (τ_2), stimulated emission can only be observed if $\tau_s < \tau_2$. Our previous studies (*14*) indicate that τ_2 scales with dot size as R^3 ($\tau_2 \approx \beta R^3$, where $\beta \sim 5$ ps nm^{-3}). This result, along with Eq. 1, allows us to write the following threshold condition for the observation of stimulated emission in QD samples

$$\xi\sigma_g > \frac{4\pi n_r}{3c\beta} \qquad (2)$$

Using $\sigma_g \approx 2 \times 10^{-17}$ cm^2 measured for the 1.3-nm dots, we obtain $\xi > 0.002$. In glass samples, ξ is usually <0.001. This may explain why, despite observations of optical gain, stimulated emission was not realized in strongly confined QDs made in glasses. The volume fraction of dots is substantially higher in close-packed QD films. For example, for films made of TOPO-capped 1.3-nm QDs, ξ is ~0.20, assuming random close packing. For such high packing densities, the condition given by Eq. 2 is easily satisfied. This indicates that stimulated emission should be observed in samples of close-packed QD solids, provided that the optical quality of the sample is sufficiently high so that the gain can overcome optical losses from scattering.

We compared gain spectra at room and liquid nitrogen temperatures. As expected for strongly confined QDs, the gain threshold is nearly temperature-independent. The maximum gain observed at cryogenic temperatures was slightly higher than that at room temperature,

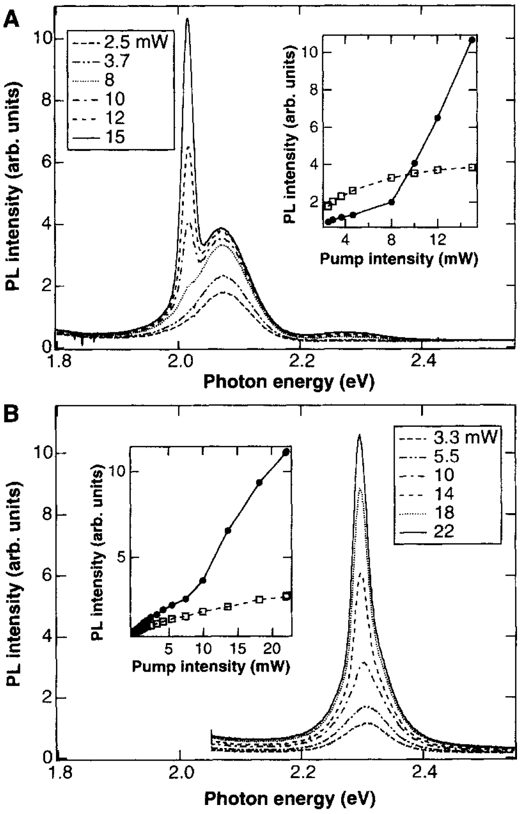

Fig. 4. Development of a sharp stimulated emission band as a function of pump intensity in PL spectra of films (T = 80 K) fabricated from (**A**) TOPO-capped QDs with R = 2.1 nm and (**B**) ZnS-capped QDs with R = 1.35 nm. (Insets) Superlinear intensity dependence of the stimulated emission (circles) showing a clear threshold compared to the sublinear dependence of the PL intensity outside the sharp stimulated emission peak (squares).

primarily the result of a higher threshold for film optical damage at low temperature. Higher film stability at low temperatures likely explains the fact that, although we observed gain at both room and cryogenic temperatures, the clear signatures of stimulated emission were only detected at temperature $T = 80$ K. Figure 4 shows examples of stimulated emission spectra for close-packed films of TOPO-capped QDs with $R = 2.1$ nm (Fig. 4A) and ZnS-capped QDs with $R = 1.35$ nm (Fig. 4B), recorded at progressively higher pump levels. The films are optically pumped perpendicular to the sample plane, and the stimulated emission is detected at the edge of the films that act as optical waveguides. The development of a sharp stimulated emission peak is observed in both examples at wavelengths characteristic for the dot size, highlighting the size-controlled spectral tunability of the stimulated emission with dot size. The pump intensity dependence of this peak (Fig. 4, insets) shows a threshold behavior that is a clear signature of optical amplification. TOPO-capped QDs have poorer surface passivation and hence substantially smaller PL quantum yield than ZnS-capped dots. Nevertheless, because the Auger time scale is substantially faster than surface trapping in these dots, both types of samples showed similar gain properties.

Not all of the films that showed an optical gain in TA measurements demonstrated stimulated emission in PL spectra. This was probably due to differences in the optical quality of the films in their lateral directions. Images of QD samples taken with an optical microscope show chaotic networks of cracks on a sub–20-μm length scale. The surface density of cracks varied from sample to sample, leading to substantial differences in optical scattering losses in the lateral directions (across the cracks) for the millimeter lengths required for achieving large optical amplifications. Such differences in optical losses are much less pronounced in TA measurements where the samples are probed in a vertical direction (along the cracks) with the path length limited to 0.3 to 2 μm.

We demonstrated room and low-temperature optical gain in strongly confined nanocrystal QDs assembled as close-packed films (QD solids). Narrowband stimulated emission that is spectrally tunable with dot size and has a clear threshold behavior was also demonstrated for films cooled to liquid nitrogen temperature. These results provide a proof of principle for lasing in strongly confined nanocrystal QDs and should motivate the development of nanocrystal QD-based lasers and amplifiers over a broad spectral range.

Note added in proof: Recently, we were able to demonstrate room temperature narrowband stimulated emission in CdSe QD films.

References and Notes

1. D. Mehus and D. Evans, *Laser Focus World* **31**, 117 (1995).
2. A. Strass, *Laser Focus World* **30**, 79 (1994).
3. Y. Arakawa and H. Sakaki, *Appl. Phys. Lett.* **40**, 939 (1982).
4. M. Asada, Y. Miyamoto, Y. Suematsu, *IEEE J. Quantum Electron.* **QE-22**, 1915 (1986).
5. Al. L. Efros and A. L. Efros, *Sov. Phys. Semicond.* **16**, 772 (1982).
6. L. Brus, *J. Chem. Phys.* **79**, 5566 (1983).
7. N. N. Lebedson *et al.*, *Semiconductors* **28**, 832 (1994).
8. N. Kistaedter *et al.*, *Electron. Lett.* **30**, 1416 (1994).
9. M. Grundman, *Physica E* **5**, 167 (2000).
10. C. B. Murray, D. J. Norris, M. G. Bawendi, *J. Am. Chem. Soc.* **115**, 8706 (1993).
11. C. B. Murray, C. R. Kagan, M. G. Bawendi, *Science* **270**, 1335 (1995).
12. M. Nirmal *et al.*, *Phys. Rev. Lett.* **75**, 3728 (1995).
13. D. J. Norris, Al. L. Efros, M. Rosen, M. G. Bawendi, *Phys. Rev. B* **53**, 16347 (1996).
14. V. I. Klimov, A. A. Mikhailovsky, D. W. McBranch, C. A. Leatherdale, M. G. Bawendi, *Science* **287**, 1011 (2000).
15. V. S. Dneprovskii, V. I. Klimov, D. K. Okorokov, Yu. V. Vandyshev, *Solid State Commun.* **81**, 227 (1992).
16. J. Butty, Y. Z. Hu, N. Peyghambarian, Y. H. Kao, J. D. Mackenzie, *Appl. Phys. Lett.* **67**, 2672 (1995).
17. Y. Z. Hu, H. Gießen, N. Peyghambaeian, S. W. Koch, *Phys. Rev. B* **53**, 4814 (1996).
18. H. Gießen *et al.*, *Phase Transitions* **68**, 59 (1999).
19. M. A. Hines and P. Guyot-Sionnest, *J. Phys. Chem.* **100**, 468 (1996).
20. B. O. Dabbousi *et al.*, *J. Phys. Chem.* **101**, 9463 (1997).
21. V. I. Klimov, *J. Phys. Chem. B* **104**, 6112 (2000).
22. ——— and D. McBranch, *Phys. Rev. Lett.* **80**, 4028 (1998).
23. Sub-ps temporal resolution in the PL up-conversion experiment was achieved by gating the sample emission in the nonlinear optical crystal with a sub-ps laser pulse. The sum-frequency signal generated in the crystal is proportional to an instant PL intensity at the moment defined by an arrival time of the gating pulse. By scanning the gating pulse with respect to the PL pulse and detecting the changes in the sum-frequency signal, one can obtain information about the PL temporal profile.
24. Unless specifically mentioned, the data shown in the paper were taken at room temperature.
25. V. I. Klimov, Ch. J. Schwarz, D. W. McBranch, C. A. Leatherdale, M. G. Bawendi, *Phys. Rev. B* **60**, R2177 (1999).
26. The QDs were initially size selected and thoroughly washed by sequential precipitations from butanol, using methanol as the nonsolvent. QD solids were then prepared by drop casting films from hexane/octane solutions; solvent evaporation yielded dry solid films. The solutions were filtered immediately before film deposition to limit aggregate formation and to enhance optical quality. To further minimize aggregate formation, the solutions could be further diluted, or additional TOPO could be added. Excess TOPO, however, could also result in a loss of optical quality because the TOPO can crystallize, yielding a clouded film with a visible fractal pattern.
27. Photogenerated carrier densities were estimated with $N_{eh} = J_p\sigma_a$ where J_p is the pump fluence (photons per cm^2) and σ_a is the QD absorption cross section estimated according to (*21*).
28. This work was supported by Los Alamos Directed Research and Development funds, under the auspices of the U.S. Department of Energy; by the Air Force Office of Scientific Research, under contract MIPR-99-0026; by the NSF–Materials Research Science and Engineering Center program under grant DMR-98-08941; and by the Harrison Spectroscopy Laboratory under grant NSF-CHE-97-08265. C.A.L., H.J.E., and M.G.B. are grateful to S. Carpenter and S. Miller for technical assistance.

28 June 2000; accepted 21 August 2000

Graphite Polyhedral Crystals

Yury Gogotsi,[1]*† Joseph A. Libera,[1] Nikolay Kalashnikov,[1]
Masahiro Yoshimura[2]

Polyhedral nano- and microstructures with shapes of faceted needles, rods, rings, barrels, and double-tipped pyramids, which we call graphite polyhedral crystals (GPCs), have been discovered. They were found in pores of glassy carbon. They have nanotube cores and graphite faces, and they can exhibit unusual sevenfold, ninefold, or more complex axial symmetry. Although some are giant radially extended nanotubes, Raman spectroscopy and transmission electron microscopy suggest GPCs have a degree of perfection higher than in multiwall nanotubes of similar size. The crystals are up to 1 micrometer in cross section and 5 micrometers in length, and they can probably be grown in much larger sizes. Preliminary results suggest a high electrical conductivity, strength, and chemical stability of GPC.

Both graphite whiskers (*1*) and carbon nanotubes (*2*) represent unusual forms of carbon based on the distortion of graphene sheets. Conventional graphite forms hexagonal plate-like crystals with a very weak bonding between graphene layers. Graphite whiskers, in which a graphene sheet rolls into a scroll (*1*), provide a benchmark against which the performance of carbon fibers is compared. The discovery of carbon nanotubes (*2*) demonstrated the possibility of making strong graphite crystals consisting of coaxial closed tubes and challenged the position of whiskers as the strongest material known (*3*–*9*).

We report another form of strong filament based on graphite but with a much different structure than those reported previously. They

---

[1]University of Illinois at Chicago, Department of Mechanical Engineering, Chicago, IL 60607, USA. [2]Tokyo Institute of Technology, Materials and Structures Laboratory, 4259 Nagatsuta, Midori-ku, Yokohama 226, Japan.

*To whom correspondence should be sent: gogotsi@drexel.edu

†Present address: Drexel University, Department of Materials Engineering, Philadelphia, PA 19104, USA.